JOURNAL OF MATERIALS SCIENCE: MATERIALS IN MEDICINE 9 (1998) 347–354

Structure and strength of low-mercury dental amalgams prepared with liquid Hg–47.4% In alloy

A. FRIEDMAN, A. KAUFMAN*
IKA Materials Engineering, Sd. Itzhak 5, Haifa 34482, Israel
**E-mail: IKAL@netvision.net.il*

Two low-mercury amalgams: (1) low-copper lathe-cut and (2) high-copper (Tytin) were prepared by amalgamation with liquid Hg–47.4% In alloy. The strength–structure relationship of these amalgams was investigated and compared with standard amalgams (i.e. amalgams prepared with the same powders and pure mercury). The matrix phase of the low-mercury amalgam was found to be depleted of mercury and may be thought of as In_4Ag_9 compound with some mercury dissolved, indicating that less mercury (compared with standard amalgam) combines with silver, thus producing a strong amalgam matrix. On the other hand, an increase was observed in the consumption of the initial γ (Ag_3Sn)-phase, leading to an increase of the tin released. As a result, the potential of [HgSn]-phase formation in low-mercury amalgams increases. The observed increase in the quantity of $\gamma_2(Sn_{7-8}Hg)$-phase in low-copper amalgam, or its appearance in high-copper amalgam (where it is normally absent), contributes to a deterioration in the strength of the investigated amalgam. The conclusion drawn was that low-mercury amalgam may be prepared with liquid Hg–47.4% In alloy but, in order to eliminate γ_2-phase formation, novel and possibly tin-free amalgamable alloys should be developed.

1. Introduction

Modern dental amalgams contain approximately 41%–54% mercury [1]. Although, throughout the history of dental amalgam, no adverse health effects have been reported, the present trend is to reduce to a minimum the amount of mercury in these alloys. Because, moreover, a significant portion of mercury from amalgam scrap reaches the soil, that trend is gaining in importance.

The amalgamation reaction in dental amalgam may be considered as a liquid sintering process which requires a certain volume ratio between the solid and the liquid phases. This requirement and the quality of the freshly triturated amalgam slurry determine the actual mercury content in dental amalgams.

One of the ways to provide the required amount of liquid phase while using less mercury is to use alloyed, instead of pure, mercury. Indium is a most suitable candidate for alloying of mercury. According to the equilibrium Hg–In phase diagram [2], up to 54% by weight of indium may be dissolved in mercury at room temperature. In addition, indium is non-toxic and forms intermetallic compounds with the main amalgamable alloy components such as silver and tin.

As early as 1977, admixing of unalloyed indium powder to amalgamable alloy powder was proposed [3]. As was mentioned in the relevant patent, indium powder readily reacts with mercury during trituration and forms liquid Hg–In alloy before significant amalgamation of the amalgamable alloy powder occurs. That is why the initial ratio between amalgamable powder and mercury may be increased, reducing the mercury content in the resultant amalgam. Studies of the amalgam prepared by the above method [4, 5] have shown that admixed indium significantly decreases the mercury vapour release, a fact recently confirmed in dental amalgams prepared directly with Hg–In liquid alloys [6].

The compressive strength of the indium-containing amalgams, prepared by either of the methods described, has also been investigated [6–10]. It was reported [6, 9,10] that indium decreases the setting rate, which in turn affects the 1 h compressive strength of the amalgam. For example, as recently reported by Okabe *et al.* [6], the ANSI/ADA Specification minimum value of 80 MPa for that strength was exceeded only by an amalgam prepared with liquid Hg–10% In alloy.

At small quantities of incorporated indium, the 24 h and 7 d compressive strengths did not drop and even increased over that of the commercial amalgams [7, 8, 10]. However, when the amount of incorporated indium is increased, the 24 h and 7 d compressive strengths begin to drop [8, 9]. For example, according to data given by Hero *et al.* [9] the 24 h compressive strength of amalgam prepared with Duralloy® commercial amalgamable alloy powder and liquid Hg–18.8% In (by weight) alloy did not meet the minimum pertinent standard requirement of 300 MPa.

While the initial setting rate of indium-containing amalgam may be increased by, for example, incorporating foreign particles, which facilitates nucleation of

0957–4530

the amalgam phases, or by utilizing a finer powder of the amalgamable alloy, the 24 h and 7 d compressive strengths generally relate to the amalgam's structure. The only relevant data were presented by Hero *et al.* [11]. In that work it was found that when amalgamating Duralloy® powder with liquid Hg–18.8% In alloy, the matrix (γ_1-phase) of the resultant amalgam contained 7 at % In. In addition, in that case no unconsumed amalgamable alloy particles were found. The decrease of the amalgam's compressive strength was explained by enhanced embrittlement of the matrix (γ_1-phase) due to dissolution of indium.

To diminish significantly mercury contamination of the environment, low-mercury amalgams, containing less than 25% Hg, should be developed. This may be achieved by utilizing liquid Hg–In alloys with a high indium content ($\sim$50% In by weight).

The objective of the present work was a structure-to-strength relationship investigation of two low-mercury amalgams: (1) low-copper lathe-cut, and (2) high-copper (Tytin), prepared with liquid Hg–47.4% In alloy. The corresponding standard amalgams (i.e. amalgams prepared with the same amalgamable powders and pure mercury) were also tested for comparison. The choice of the amalgamable powders for investigation was prompted by two considerations: low-copper lathe-cut amalgamable powder is a constituent of a great number of high-copper dispersant amalgams, and Tytin is a widely used modern high-copper single composition amalgam.

2. Materials and methods

The low-copper amalgam was prepared with conventional zinc-free lathe-cut powder Silmet 68% medium setting non-zinc, Elite-Scientific Metal Co. Ltd, manufactured by Silmet and liquid Hg–47.4% In (by weight) alloy. The Silmet powder contains 68% Ag, 26% Sn, and 6% Cu and has a particle size of 5–53 μm. The high-copper amalgam was prepared with commercial amalgamable powder Tytin (S.S. White Ltd, USA), normally comprising 60% Ag, 27% Sn, 13% Cu, and the above liquid alloy. The liquid Hg–47.4% In alloy was prepared by heating pure mercury (99.999%) and pure indium (99.999%) in hermetic stainless steel containers.

The data on amalgam preparation are listed in Table I.

After trituration the amalgams were condensed in accordance with ISO 1559 : 1986 requirements, and cylindrical samples (4 mm diameter, 8 mm long) were prepared. The compressive strength of the amalgams was measured in an Instron testing machine after 24 h ageing at 37 °C, the average value representing five specimens tested being tabulated. For microstructural investigation, the samples, after a minimum of 2 wk storage at 37 °C, were mounted in rings using room-temperature-curing epoxy resin, and metallographic sections were prepared at low stress. The samples were examined under a Jeol-840 scanning electron microscope (SEM) equipped with a LINK-ISIS energy-dispersive spectroscopy (EDS) analyser within 1 h of polishing or after polishing and light etching by the double-etch technique developed by Wing [12]. Five separate areas were analysed for each phase. The rest of the cylindrical amalgam samples were ground into powders for the X-ray diffraction measurements with a Siemens D-5000 diffractometer delivering CuK_α radiation. Data for all the samples were collected by step scan, 0.02° per 9 s step. $Ag_3Sn(\gamma)$ and $Sn_{7-8}Hg(\gamma_2)$ phases were identified with the aid of Fairhurst and co-workers data [13, 14], and the rest of the phases present, by comparison with the JCPDS card file data. The corresponding file numbers are presented in Table II.

TABLE II The numbers of JCPDS card files utilized for identifying individual amalgam phases

Phase	JCPDS card file number
$\gamma_1(Ag_2Hg_3)$	11-0067
$\eta'(Sn_5Cu_6)$	2-0713
Cu_3Sn	1-1240
In_4Ag_9	29-0678

The matrix-phase lattice constant was determined by computer-fitting the reflection peaks using the least-squares method. Peaks belonging to more than one phase were eliminated from the calculation.

3. Results and discussion

The 24 h compressive strength data, presented in Table III, show a sharp drop in the values for low-mercury amalgams. The result obtained coincides with the literature data [8, 9]. The microstructures of the low-copper lathe-cut standard and of the low-mercury amalgams are presented in Figs 1 and 2, respectively. As can be seen in Fig. 1, all main phases are present in the standard amalgam structure. The general structure of the low-mercury amalgam

TABLE I Data on amalgam preparation

Amalgam	Powder	Liquid alloy composition (wt %)		Liquid-to-solid ratio	Trituration time (s) high-speed amalgamator
		Hg	In		
Low-Cu standard	Low-copper lathe-cut	100	0	1/1	6
Low-Cu, low-Hg	Low-copper lathe-cut	52.6	47.4	0.8/1	6
High-Cu standard	High-copper Tytin	100	0	0.8/1	6
High-Cu, low-Hg	High-copper Tytin	52.6	47.4	0.7/1	6

TABLE III 24 h compressive strength

Amalgam	24 h compressive strength (MPa)
Low-Cu standard	310
Low-Cu, low-Hg	135
High-Cu standard	434
High-Cu, low-Hg	190

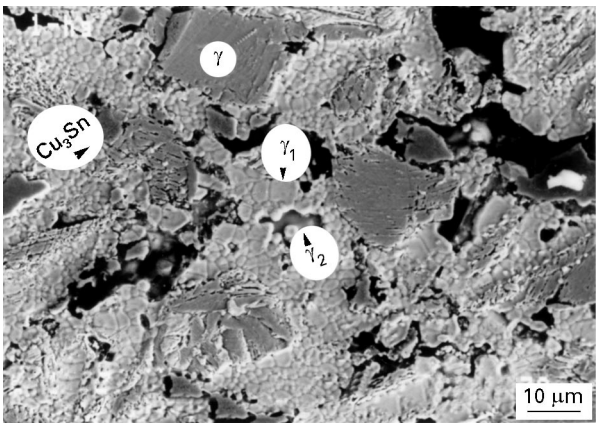

Figure 1 Scanning electron micrograph of amalgam made with pure mercury and low-copper lathe-cut powder. Double etching.

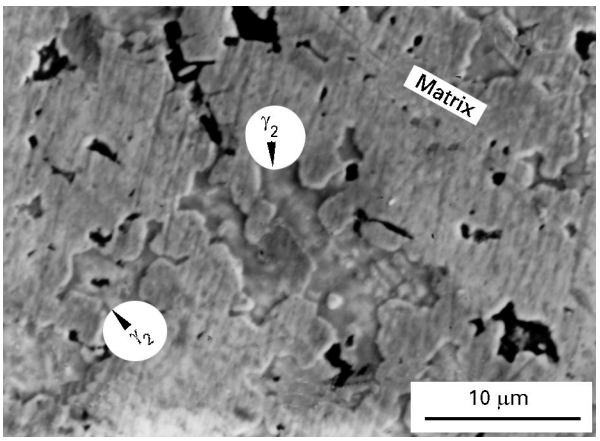

Figure 2 Scanning electron micrograph of amalgam made with low-copper lathe-cut powder and liquid Hg–47.4% In alloy. As-polished.

(presented in Fig. 2) is different from that of Fig. 1. No unconsumed lathe-cut particles were found. A small quantity of Cu_3Sn particles and large γ_2 areas were found embedded in the amalgam matrix. Double etching did not reveal the matrix-phase grain structure. The EDS analysis results of both amalgams are presented in Tables IV and V and will be discussed below together with the X-ray diffraction analysis data.

3.1. Matrix phase

The data in Table IV shows that the matrix-phase composition of the standard low-copper amalgam is close to the conventional formula, $Ag_{22}SnHg_{27}$ [15]. The presence of some copper in the unetched sample matrix may be due to a small amount of η'-phase (Sn_5Cu_6), which is present throughout the γ_1-matrix. In contrast, the matrix composition of the relevant low-mercury amalgam (Table V) approaches that of the intermetallic compound In_4Ag_9 (existing in the Ag–In binary system [16]). The increased silver content and the decreased mercury content in the amalgam matrix with an increase of incorporated indium can be found in the relevant literature [11, 17]. Literature and our data on [Ag Hg In]-phase chemical composition, are presented in Table VI.

The lattice constants of the matrix phase of the low-copper lathe-cut standard and low-mercury amalgams measured in the present work are presented in Table VII and compared with the JCPDS card file data for the compounds Ag_2Hg_3 and In_4Ag_9.

As can be seen, the low-mercury amalgam matrix phase has a lattice constant lower than that of the standard amalgam. The observed decrease of the lattice constant may be explained by the fact that the silver content in the matrix phase of the low-mercury amalgam significantly increases (silver having an atomic volume considerably smaller than that of indium and mercury: 10.28, 15.71 and 14.81 cm^3 $g\text{-}atom^{-1}$, respectively [18]). While the matrix phase of the standard low-copper amalgam may be described as Ag_2Hg_3 compound, and more exactly as $Ag_{11}Hg_{15}$ [19] with a small amount of dissolved tin, the matrix phase of the amalgam prepared with liquid Hg–47.4% In alloy may be described as In_4Ag_9 compound containing some dissolved mercury. Both intermetallic compounds discussed have a cubic crystal structure, and the difference between their lattice constants is not large, which is why a continuous range of solid solutions between them can be formed. This means that dissolution of indium in the amalgam

TABLE IV Standard low-copper amalgam. Results of EDS analysis

Phase	Analysed area	Chemical composition (at %)			
		Ag	Sn	Cu	Hg
$Ag_3Sn(\gamma)$, unconsumed	As-polished sample	71.0 ± 0.5	23.9 ± 0.4	2.7 ± 0.3	2.4 ± 0.1
Ag_3Sn, calc.	–	75	25	–	–
Cu_3Sn	As-polished sample	1.2 ± 0.2	29.7 ± 0.4	68.7 ± 0.9	0.4 ± 0.1
Cu_3Sn, calc.	–	–	25	75	–
Matrix (γ_1)	As-polished sample	40.9 ± 0.5	1.8 ± 0.3	3.5 ± 0.5	53.8 ± 0.3
	Large grains after light etching	41.1 ± 0.6	2.1 ± 0.4	1.3 ± 0.8	55.6 ± 0.5
$Ag_{22}SnHg_{27}$, calc.	–	44	2	–	54
γ_2	After light etching	0	87.8 ± 0.8	0.5 ± 0.5	11.7 ± 0.3
$Sn_{7-8}Hg$, calc.	–	–	87.5–89.0	–	11.0–12.5

TABLE V EDS analysis of the low-copper amalgam prepared with liquid Hg–47.4% In alloy

Phase	Analysed area	Chemical composition (at %)				
		Ag	Sn	Cu	Hg	In
Cu_3Sn	As-polished	0.8 ± 0.2	28.8 ± 0.3	69.2 ± 0.7	0.3 ± 0.1	0.8 ± 0.3
Cu_3Sn, calc.	–	–	25	75	–	
Matrix phase	As-polished	63.6 ± 0.6	0	0.6 ± 0.6	10.9 ± 0.2	24.9 ± 0.7
$Ag_{22}SnHg_{27}$, calc.	–	44	2	–	54	–
In_4Ag_9 [16]		66.5–69.0	–	–	–	31.0–33.5
γ_2	As-polished sample	0.7 ± 0.4	82.2 ± 0.7	0.8 ± 0.4	9.7 ± 0.2	6.5 ± 0.5
$Sn_{7-8}Hg$, calc.	–	–	87.5–89.0	–	11.0–12.5	–

TABLE VI [AgHgIn]-phase composition of the various indium-containing amalgams (standard deviation is not shown)

Alloy	Chemical composition (at %) of [AgHgIn]-phase					Source
	Ag	Hg	In	Cu	Sn	
$Ag_{11}Hg_{15}$	43.2–44.3	55.7–56.8	–	–	–	[19]
Standard amalgam prepared with "Indiloy" 4.4% In (wt) in prealloyed powder	47.6	48.8	1.9	0	1.7	[17]
Amalgam prepared with low-Cu lathe-cut powder and liquid Hg–10% In (wt) alloy	47.0	47.3	4.2	0.6	0.9	Own data, unpub.
Duralloy® prepared with liquid Hg–11.1% In (wt) alloy	51	45	4	1	0	[11]
Duralloy® prepared with liquid Hg–18.8% In (wt) alloy	54	38	7	2	0	[11]
Amalgam prepared with low-Cu lathe-cut powder and liquid Hg–20% In (wt) alloy	52.9	35.4	10.5	1.0	0.1	Own data, unpub.
Amalgam prepared with low-Cu lathe-cut powder and liquid Hg–47.4% In (wt) alloy	63.6	10.9	24.9	0.6	0	Present work
Diffusion layer formed after 1 mon immersion of Ag particles in liquid Hg–47.4% In (wt) alloy at 37 °C	65.8	3.0	31.2	–	–	Own data unpub.
In_4Ag_9	66.5–69.0	–	31.0–33.5	–	–	[16]

TABLE VII Lattice constants of the matrix phase

Amalgam (intermetallic compound)	Range of angles	Number of peaks	Lattice constant (nm)
Ag_2Hg_3 (JCPDS, file 11-0067)	–	–	1.0040
Amalgam prepared with low-Cu lathe-cut powder and pure Hg	$21^\circ < 2\theta < 137^\circ$	42	1.0036(1)
Amalgam prepared with low-Cu lathe-cut powder and liquid Hg–47.4% In alloy	$31^\circ < 2\theta < 112^\circ$	23	0.9913(1)
In_4Ag_9(JCPDS, file 29-0678)	–	–	0.9922

matrix will always be followed by an increase of its silver, and a decrease of its mercury content. Furthermore, the Ag–Hg–In ratio will be so arranged that the points denoting the chemical composition of the matrix phase in the Ag–Hg–In concentration triangle will be lined up approximately along the straight line connecting the binary intermetallic compounds $Ag_{11}Hg_{15}$ and In_4Ag_9.

The ternary Ag–Hg–In equilibrium diagram is not available. To confirm the above assumptions, the chemical compositions of the indium-containing amalgam matrix listed in Table VI were plotted on the appropriate concentration triangle (Fig. 3).

To express the chemical composition of the matrix, the data in Table VI were corrected for 100% total silver, indium and mercury content.

The data presented in Fig. 3 indicate the consistency of our assumptions. The scattering of the experimental points may be due to EDS analysis errors as well as to the existence of the [AgHgIn]-phase homogeneity field.

3.2. γ_2 phase

The Sn–Hg equilibrium phase diagram [20] (Fig. 4) shows that both intermetallic compounds (marked γ and δ) relevant to the dental amalgam field are located in a very narrow range of concentrations. In addition, each of the phases discussed has its own narrow range of homogeneity, while the relevant phase boundaries are not precisely established.

Some of the data in the literature relating to the presence of the above-mentioned phases in dental amalgam, will now be briefly discussed. In accordance with the results obtained by Fairhurst and Ryge [14] γ-phase (termed γ_2 in the dental literature) is the only

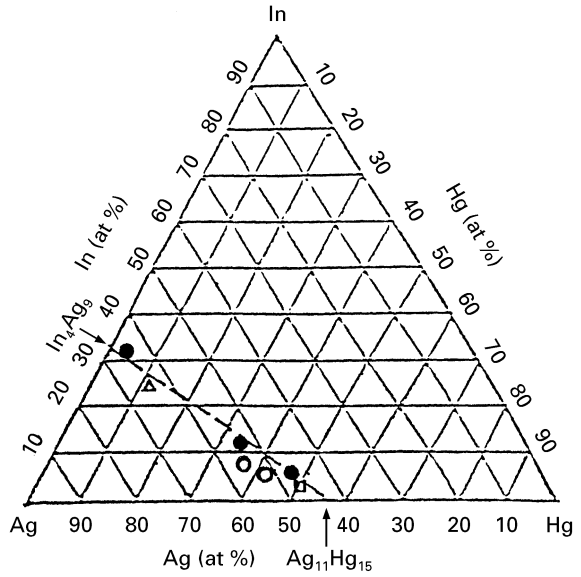

Figure 3 Ag–In–Hg concentration triangle with various measured chemical compositions of the matrix phase. (□) Mahler and Adey [17], (●) own data (unpublished), (○) Hero *et al.* [11], (▽) present work.

tin–mercury phase that may be present in a dental amalgam structure. That phase has a hexagonal unit cell and a homogeneity range of 11.0–12.5 at % Hg, which corresponds to the $S_{7-8}Hg$ formula. Later Soderholm [21], using a precise XRD method, showed that in the tin–mercury system the hexagonal γ_2-phase field exists only up to 9.5 at % Hg, the δ-phase field starts with 12.9% Hg, and the $\gamma_2 + \delta$ field ought to be between 9.5 and 12.9 at % Hg. The δ-phase has an orthorhombic structure with a diffraction pattern almost identical to that of the γ_2-phase. Soderholm failed to separate the diffraction patterns in the two-phase ($\gamma_2 + \delta$) field. Neither calculated nor observed relative intensities of δ-phase peaks were presented. Based on the obtained results, Soderholm concluded that "the diffraction patterns identified as being due to the γ_2-phase in most articles could also be due to the δ-phase". Sarkar's thermal analysis [22] discovered endothermic peaks at $\sim 90\,^{\circ}C$ when heating some of the commercial dental amalgams. The peaks were interpreted as being related to δ-phase decomposition. Endothermic peaks at similar temperatures were obtained by Matsuda *et al.* [23] when heating the mixtures of separately prepared amalgam phases γ, γ_1, and γ_2. They concluded that the $\gamma_1 + \gamma_2 \rightarrow \beta_1$ reaction is responsible for the low-temperature endothermic peaks in low-copper amalgams and $\gamma_1 + \gamma \rightarrow \beta_1$ is responsible for them in high-copper amalgams.

To ascertain the actual situation, a precise X-ray diffractometric analysis should be conducted on commercial dental amalgams (but not on binary Hg–Sn alloys) in combination with its thermal analysis.

In the present work, the most important point was that both Hg–Sn phases reviewed are mechanically weak and deteriorate the dental amalgam strength.

No separation of γ and δ phase spectra was found in our experiments. The Hg–Sn phase diffraction peaks were satisfactorily indexed on the assumption that the unit cell is hexagonal. We compared the *d*-spacings obtained for standard low-copper amalgam with

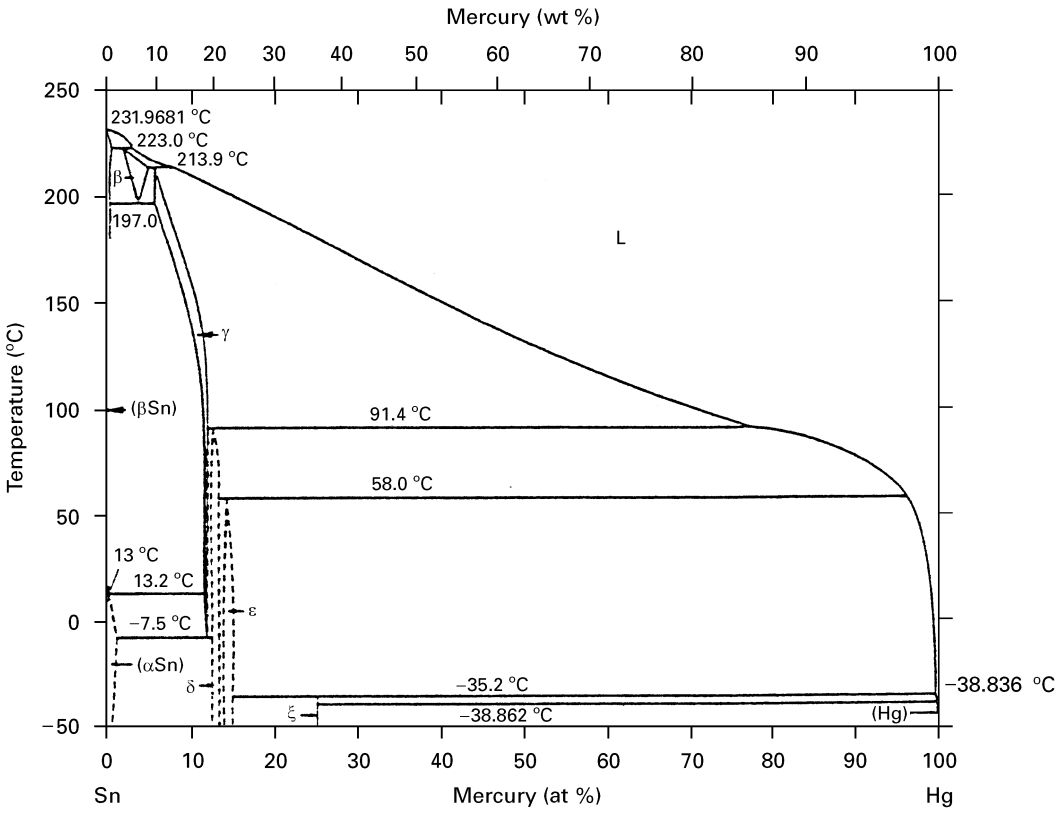

Figure 4 Hg–Sn equilibrium phase diagram.

TABLE VIII Comparison of XRD data for standard low-copper amalgam [HgSn]-phase, with literature data

Hexagonal γ_2-phase of Sn–9.5% Hg (at) alloy [21]		[HgSn]-phase of standard low-Cu amalgam[a]	Orthorhombic δ-phase of Sn–12.9% Hg (at) alloy [21]	
h k l	*d* (nm)	*d* (nm)	*h k l*	*d* (nm)
0 0 1	0.298 764	0.2987	0 0 1	0.298 560
1 0 0	0.277 859	0.2779	2 0 0	0.277 501
–	–	–	1 1 0	0.276 013
1 0 1	0.203 465	0.2034	2 0 1	0.203 149
1 1 0	0.160 417	0.1604	–	0.160 229
0 0 2	0.149 345	0.1494	0 0 2	0.149 260
1 1 1	0.141 342	0.1413	–	0.141 170
–	–	–	0 2 1	0.140 525
2 0 0	0.138 949	0.1390	4 0 0	0.138 110
–	–	–	0 1 2	0.135 076
1 0 2	0.131 527	0.1316	2 0 2	0.131 441
2 0 1	0.125 955	–	4 0 1	0.125 806
1 1 2	0.109 324	0.1094	–	–
1 2 0	–	0.1050	–	–

[a] [HgSn]-phase peaks coincident with those relating to other amalgam phases are eliminated from the tabulation.

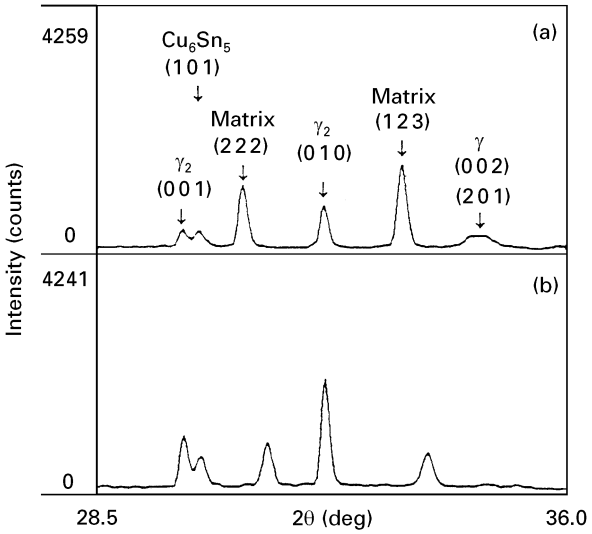

Figure 5 The $28.5^\circ < 2\theta < 36^\circ$ portion of the X-ray diffraction patterns of (a) standard low-copper amalgam and (b) amalgam prepared with liquid Hg–47.4% In alloy. The spectra have been computer-smoothed with the "linear smooth" algorithm.

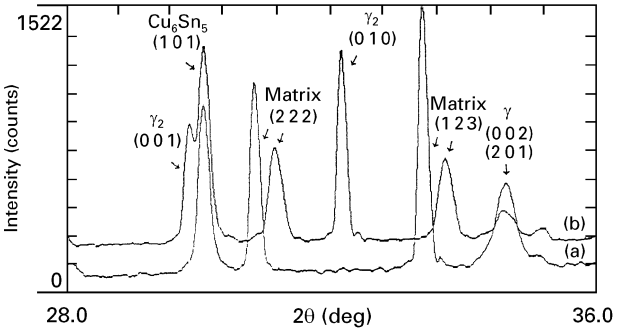

Figure 6 The $28.5^\circ < 2\theta < 36^\circ$ portion of the X-ray diffraction patterns of (a) standard Tytin amalgam and (b) low-mercury Tytin amalgam prepared with liquid Hg–47.4% In alloy. The spectra have been computer-smoothed with the "linear smooth" algorithm.

those of Soderholm [21] for γ_2-phase (an alloy containing 9.5 at % Hg), and for δ-phase (an alloy containing 12.9 at % Hg). The relevant data, presented in Table VIII, clearly shows that the *d*-spacings we measured are in complete accord with the hexagonal structure.

The portion of the X-ray diffraction pattern in the range of angles, $28.5^\circ < 2\theta < 36.0^\circ$, obtained for the standard low-copper amalgam and for the amalgam prepared with liquid Hg–47.4% In alloy, is presented in Fig. 5. That portion comprises (0 0 1) and (1 0 0) peaks of the γ_2-phase. As can be seen, the intensity of the peaks is significantly higher for the latter amalgam. Our XRD-method was not quantitative, but all the samples were tested at the same settings of the X-ray diffractometer, and the results obtained, therefore, indicate a significant increase in the quantity of the mechanically weak γ_2-phase in the structure of low-mercury amalgam. To confirm the revealed influence of liquid Hg–47.4% In alloy on low-copper lathe-cut powder amalgamation, high-copper amalgam Tytin, prepared with the same liquid Hg–In alloy, was also investigated and compared with standard Tytin amalgam. The portion of the X-ray diffraction pattern in approximately the same range of angles ($28^\circ < 2\theta < 36^\circ$), obtained for standard and low-mercury amalgam Tytin, is shown in Fig. 6. While the results obtained confirm the well-known fact of γ_2-phase absence in standard amalgam Tytin (no (0 0 1) and (0 1 0) γ_2-phase peaks were found in the range mentioned), two of its strong peaks can be seen in the spectrum of low-mercury Tytin.

3.3. Ag_3Sn(γ)-phase

The absence of unconsumed γ-phase particles in the structure of the low-copper amalgam prepared with liquid Hg–47.4% In alloy is confirmed by X-ray diffraction analysis. For example, in Fig. 5, a small peak of the γ-phase is present in the spectrum of standard

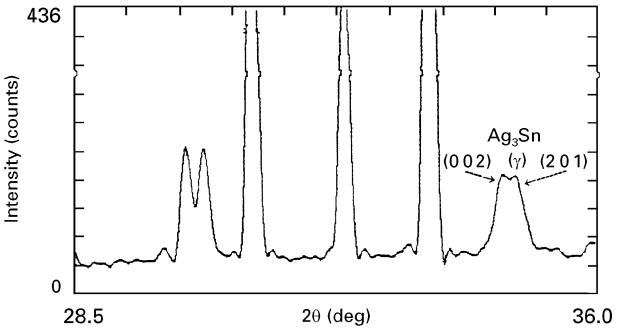

Figure 7 The $28.5^\circ < 2\theta < 36^\circ$ portion of the X-ray diffraction pattern of standard amalgam (as in Fig. 5). The high-intensity peaks have been cut in order to emphasize the small ones. The spectrum has been computer-smoothed by the "linear smooth" algorithm.

amalgam but is absent from the spectrum of the amalgam prepared with liquid Hg–47.4% In alloy. In order to emphasize the small γ-phase peak, the high-intensity peaks in Fig. 5 have been cut. The resulting fragmentary image obtained for standard amalgam, depicted in Fig. 7, shows two γ-phase peaks superimposed. In accord with Fairhurst and Cohen [13], the peaks discussed may be indexed as (0 0 2) and (2 0 1). A reduced γ-phase in low-mercury Tytin may also be seen in the spectrum of Fig. 6, when comparing the (0 0 2), (2 0 1) peak for both amalgams. The results obtained coincide with Hero's data [11], which demonstrate the absence of unconsumed γ-phase in the structure of an amalgam prepared with Duralloy® powder and liquid Hg–18.8% In alloy. The findings indicate that, compared with the standard practice (amalgamation with pure mercury), more tin is released when amalgamating with liquid Hg–In alloys.

3.4. Cu_6Sn_5- and Cu_3Sn-phases

Cu_6Sn_5-phase peaks were observed in the X-ray diffraction spectra of all the amalgams investigated. For example, the (1 0 1) peak of that phase (according to JCPDS file 2-0713, it is of 100% intensity) may be seen in Figs 5 and 6. Its presence in the low-copper amalgams has been reported previously [24].

In accordance with our metallographic and EDS analysis results, Cu_3Sn-phase particles are present in the structure of both low-copper amalgams. Because of the relatively small amount of Cu_3Sn-phase and the fact that its 100% intensity peak is coincident with that of Cu_6Sn_5-phase, its X-ray diffraction analysis could not produce specific results for the amalgams investigated.

3.5. Other phases

No undissolved indium particles were found in the low-mercury amalgam structure. All peaks present in the X-ray diffraction spectra were identified as being related to the phases discussed.

4. Conclusions

The findings relating to the γ, γ_2 and matrix phases of low-mercury amalgams correspond well with each other. An increase in the consumption of the initial amalgamable powder, when being amalgamated with liquid Hg–47.4% In alloy, leads to an increase in the amount of tin released. On the other hand, less mercury (compared with standard amalgam) is combined with silver in the low-mercury amalgam matrix (low-mercury amalgam matrix contains only $\sim$11 at % Hg, while for the standard type, the corresponding value is $\sim$55 at %). As a result, tin combines with unconsumed mercury, forming the mechanically weak [HgSn]-phase. The observed increase in γ_2-phase (low-copper amalgam), or its appearance (high-copper amalgam Tytin), contributes to the deterioration in strength of the low-mercury amalgams.

The main conclusion is that low-mercury amalgam may be prepared with liquid Hg–47.4% In alloy, but in order to eliminate γ_2-phase formation, novel and possibly tin-free, amalgamable alloys should be developed.

Acknowledgements

Collaboration with and the support of Silmet Ltd, and a Grant from the Ministry of Commerce and Industry (Israel) are gratefully acknowledged.

References

1. M. A. COCHRAN and E. S. DUKE, *J. Indiana. Dent. Assoc.* **60** (1981) 2.
2. T. B. MASSALSKY (ed.), in "Binary Alloys Phase Diagrams", Vol. 3, 2nd Edn (ASM International, 1992) pp. 2130, 2132, 2133.
3. W. V. YOUDELIS, inventor, "Dental powder composite and amalgam", US Pat. 4039 329, 2 August (1977).
4. *Idem*., in "Advanced Materials and Processes", Proceedings of the First European Conference EUROMAT 89, Vol. 2, "High Technology Applications, Interfaces and Related Topics", edited by K. E. Exner and V. Schumacher (DGM Informationsgesellschaft, Olerursel, 1990) p. 785.
5. L. V. POWELL, G. H. JOHNSON and D. J. BALES, *J. Dent. Res.* **68** (1989) 1231.
6. T. OKABE, T. YAMASHITA, H. NAKAJIMA, A. BERGLUND, L. ZHAO, I. GUO and J. L. FERRACANE, *J. Dent. Res.* **73** (1994) 1711.
7. W. V. YOUDELIS, *J. Canad. Dent. Assoc.* **2** (1979) 64.
8. H. J. MUELLER and E. M. NAREA, in "Transactions of the Eleventh Annual Meeting of the Society for Biomaterials", San Diego, April 1985, p. 59.
9. H. HERO, R. B. JORGENSEN and L. SHUIPING, *J. Dent. Res.* **73**, IDAR Abstracts, abst. 29 (1994) 105.
10. G. H. JOHNSON and L. V. POWELL, *Dent. Mater.* **8** (1992) 366.
11. H. HERO, R. B. JORGENSEN and L. SHUIPING, *Biomaterials* **16** (1995) 581.
12. G. WING, *Austral. Dent. J.* **4** (1965) 113.
13. C. W. FAIRHURST and J. B. COHEN, *Acta Crystallogr.* **B28** (1972) 371.
14. C. W. FAIRHURST and G. RYGE, *Adv. X-ray Anal.* **5** (1962) 64.
15. D. B. MAHLER and J. D. ADEY, *J. Dent. Res.* **54** (1975) 218.
16. T. B. MASSALSKY (ed.), in "Binary Alloys Phase Diagrams", Vol. 2, 2nd Edn (ASM International, Metals Park, Ohio, 1992) 1481.

17. D. B. MAHLER and J. D. ADEY, *J. Dent. Res.* **63** (1984) 921.
18. T. LYMAN, (ed.), "Metals Handbook", Vol. 1, 8th Edn (ASM, Metals Park, 1964) p. 44.
19. T. B. MASSALSKY (ed.), in "Binary Alloys Phase Diagrams", Vol. 1, 2nd Edn (ASM International, Metals Park, Ohio, 1992) p. 43.
20. *Idem*, *ibid*., Vol. 3, p. 2168.
21. K. J. SODERHOLM, *J. Dent. Res.* **3** (1987) 713.
22. N. K. SARKAR, *J. Mater. Sci. Mater. Med.* **5** (1994) 171.
23. K. MATSUDA, H. OHMO, T. HAMAWA, J. L. FERRACAME, R. SPEARS and T. OKABE, *J. Dent. Res.* **66**, IDAR Abstracts, abst. 1469 (1986) 290.
24. S. L. JENSEN, *Scan. J. Dent. Res.* **80** (1972) 158.

Received 4 March
and accepted 5 September 1997